Heat generation in Nd doped vanadate crystals with 1.34 μm laser action

Masahito Okida, Masahide Itoh, Toyohiko Yatagai

Institute of Applied Physics, University of Tsukuba 1-1-1, Tennodai, Tsukuba, Ibaraki, 305-8573, Japan

Hamish Ogilvy, James Piper

Centre for Laser and Applications, Macquarie University, NSW 2109, Sydney, Australia

Takashige Omatsu

Department of Information and Image Science, Chiba University 1-33 Yayoi-cho, Inage-ku, Chiba, 263-0022

omatsu@faculty.chiba-u.jp

Abstract: Thermal load in Nd^{3+} doped vanadate crystals with and without laser action at 1.34 μm is investigated. Excited state absorption contributes significantly to a fractional thermal loading as well as quantum defect.

OCIS codes: (140.6810) Thermal effects; (140.3580) Lasers, solid-state; (140.3480) Lasers, diode-pumped

References and links

1. A. Di lieto, P. Minguzzi, A. Piratsu, S. Sanguinetti, and V. Magni, "A 7-W diode-pumped Nd:YVO_4 cw laser at 1.34 μm," Appl. Phys. B **75,** 463-466 (2002).
2. Jun Liao, Jing-Liang He, Hui Liu, Hui-Tian Wang, S. N. Zhu, Y. Y. Zhu, and N. B. Ming, "Simultaneous generation of red, green, and blue quasi-continuous-wave coherent radiation based on multiple quasi-phase-matched interactions from a single, aperiodically-poled $LiTaO_3$," Appl. Phys. Lett. **82,** 3159-3161 (2003).
3. T. Jensen, V.G. Ostroumov, J.-P Meyn, G. Huber, A. I. Zagumennyi, and I. A. Shcherbakov, "Spectroscopic Characterization and Laser Performance of Diode-Laser-Pumped Nd:$GdVO_4$," Appl. Phys. B. **58,** 373-379 (1994).
4. A. W. Tucker, M. Birnbaum, C. L. Fincher, and J. W. Erler, "Stimulated-emission cross section at 1064 and 1342nm in Nd:YVO_4," J. Appl. Phys. **48,** 4907-4911 (1977).
5. Hamish Ogilvy, Michael J. Withford, Peter Dekker and James A. Piper, "Efficient diode double-end-pumped Nd:YVO_4 laser opelating at 1342 nm," Opt. Exp. **11,** 2411-2415 (2003), http://www.opticsexpress.org/abstract.cfm?URI=OPEX-11-19-2411
6. A. Minassian and M. J. Damzen, "20 W bounce geometry diode-pumped Nd:YVO_4 laser system at 1342 nm," Opt. Commun. **230,** 191-195 (2004).
7. L. Fornasiero, S. Kuck, T. Jensen. G. Huber, and B. H. T. Chai, "Excited state absorption and stimulated emission of Nd^{3+} in crystals. Part2: YVO_4, $GdVO_4$, $Sr5(PO_4)_3F$," Appl. Phys. B. **67,** 549-553 (1998).
8. Justin L. Blows, Takashige Omatsu, Judith Dawes, Helen Pask, and Mitsuhiro Tateda, "Heat generation in Nd:YVO_4 with and without laser action," IEEE Photon. Tech. Lett. **10,** 1727-1729 (1998).
9. Justin L. Blows, Judith M. Dawes, Takashige Omatsu, "Thermal lensing measurements in line-focus end-pumped neodymium yttrium aluminium garnet using holographic lateral shearing interferometry," J. Appl. Phys. **83,** 2901-2906 (1998).
10. CASIX web site, http://www.casix.com/product/Laser_Crystal_NdYVO4.htm
11. Hong Yuan Shen, Xian Lin Meng, Ge Zhang, Jian Jie Qin, Wen Liu, Li Zhu, Cheng Hui Huang, Lin Xiong Huang, and Ming Wei, "Sellmeier's equation and the expression of the thermal refractive-index coefficient for a $Nd_{0.007}Gd_{0.993}VO_4$ crystal," Appl. Opt. **43,** 955-960 (2004).
12. T. S. Lomheim, and L. G. DeShazer, "Optical-absorption intensities of trivalent neodymium in the uniaxial crystal yttrium orthovanadate," J. Appl. Phys. **49,** 5517-5522 (1978).
13. H. R. Xia, H. D. Jiang, W. Q. Zheng, G. W. Lu, X. L. Meng, H. J. Zhang. X. S. Liu, L. Zhu, and J. Y. Wang, "Optical parameters and luminescent properties of Nd:$GdVO_4$, " J. Appl. Phys. **90,** 4433-4436 (2001).

#7562 - $15.00 USD Received 23 May 2005; revised 10 June 2005; accepted 12 June 2005

14. V. Ostroumov, T. Jensen, J. –P. Meyn, and G. Huber, "Study of luminescence concentration quenching and nergy transfer upconversion in Nd-doped $LaSc_3(BO_3)_4$ and $GdVO_4$ laser crystals," J. Opt. Soc. Am. B **15,** 1052-1060 (1998).
15. CASTECH web site, http://www.castech-us.com/ndgdvo4.htm
16. Takayo Ogawa, Yoshiharu Urata, Satoshi Wada, Koichi Onodera, Hiroshi Machida, Hideaki Sagae, Mikio Higuchi, and Kohei Kodaira, "Efficient laser performance of Nd:GdVO4 crystas grown by the floating method," Opt. Lett. **28,** 2333-2335 (2003).
17. D. L. Dexter "A theory of sensitized luminescence in solids," J. Chem. Phys. **21,** 836-850 (1953).
18. Chenlin Du, Lianjie Qin, Xianlin Meng, Guibao Xu, Zhengping Wang, Xinguang Xu, Li Zhu, Bingchao Xu, and Zongshu Shao, "High-power Nd:$GdVO_4$ laser at 1.34 μm end-pumped by laser-diode-array," Opt. Commun. **212,** 177-181 (2002).
19. H. R. Xia, X. L. Meng, M. Guo, L. Zhu, H. J. Zhang, and J. Y. Wang, "Spectral parameters of Nd-doped yttrium orthovanadate crystals," J. Appl. Phys. **88,** 5134-5137 (2000).

1. Introduction

Diode-pumped solid-state lasers in the 1.3 μm region have received a lot of interest for use in various applications such as laser display, medical diagnosis and so on [1,2]. Neodymium-doped orthovanadates (Nd:$REVO_4$) are promising crystals for 1.3 μm lasers because of their relatively large stimulated emission cross-section as well as strong absorption of pumping diode frequencies [3,4]. So far, several researchers have demonstrated 1.3 μm lasers based on vanadate crystals. The slope efficiency obtained using 1.3μm vanadate lasers is limited to only 30-40 %. This is considerably lower than that obtained with 1.06 μm lasers [5,6].

In the case of 1.3 μm lasers, a large quantum defect (the energy difference between pump and laser photon) induces significant energy dissipation through heat generation in the crystal. Development of efficient 1.3μm lasers requires careful thermal management.

Recently, Fornasiero et.al. mentioned that excited state absorption (ESA) further increased a fractional thermal loading and prevented efficient laser oscillation in 1.3μm vanadate lasers [7]. They estimated the ESA cross-section for 1.3 μm photons by using a pump-probe method, however there was little discussion about the fractional thermal loading in 1.3 μm lasers.

In this paper, we present a quantitative estimate of the fractional thermal loading in 1.3 μm lasers for Nd doped vanadate crystals such as Nd:YVO_4 and Nd:$GdVO_4$ by thermal lens measurements with and without laser action.

2. Experiments

2.1 laser system

The experimental setup is shown as Fig. 1. The cavity was composed of a simple plane-parallel resonator with an end mirror and a 95 % reflective output coupler. The cavity length was about 35 mm. The Crystals used were 0.3 at.% Nd^{3+} doped, a-cut Nd:YVO_4 and Nd:$GdVO_4$ with dimensions of 4 x 4 x 7 mm^3. The 4 mm x 4 mm faces of the crystal were AR-coated for the pump wavelength of around 808 nm. The crystal was longitudinally pumped by a fiber-coupled 15 W CW 808 nm diode laser array. The wavelength of the diode was tuned, thereby maximising absorption. The diode output was focused to a spot with a radius of 350 μm on the crystal face. Figure 2 shows the experimental output power as a function of the absorbed power. The Nd:YVO_4 exhibited a slightly better performance than the Nd:$GdVO_4$. In the case of Nd:YVO_4 a slope efficiency of 22 % was obtained and the laser threshold was 1.9 W. The output power reached 1.4 W at a pump power of 8.1 W.

#7562 - $15.00 USD Received 23 May 2005; revised 10 June 2005; accepted 12 June 2005

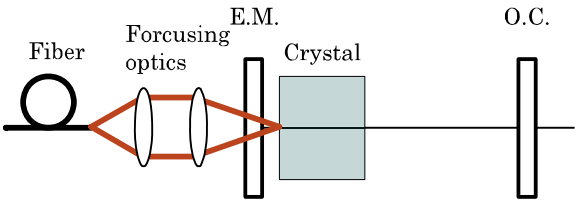

Fig. 1. Experimental setup of laser system

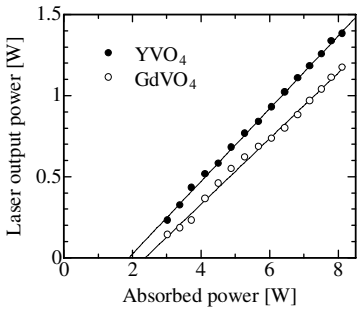

Fig. 2. Laser output power

2.2 Thermal lens measurement

To measure thermal lenses in the crystals, holographic lateral-shearing interferometry [8] was performed as shown in Fig. 3. The laser cavity was composed of an end mirror, a totally reflective 45 degree turning mirror, and an output coupler. A mechanical shutter placed inside the cavity was used to control the laser action. A green laser was used as a probe laser. The collimated probe beam made a double pass through the crystal, and the presense of thermal lens caused the wavefront of the probe beam to be distorted. After passing through the imaging optics, the distorted probe beam was directed toward the holographic shear plate. The shear plate enabled the distorted probe beam to interfere with a laterally sheared copy of itself, forming a series of fringes. By analyzing the distortion of the fringes [9], the spatial phase shift distribution $\Delta\phi(r)(= a_0 + a_1 r + a_2 r^2 + ...)$ is estimated. And then the thermal lens power D is given by

$$D = -\frac{2a_2}{k}, \tag{1}$$

where k is the wave number for 1.3 μm laser. Figure 4 shows the fringes observed with and without 1.3 μm laser actions. It is found that the distortion of fringes with laser action is significantly stronger than that without laser action.

#7562 - $15.00 USD
Received 23 May 2005; revised 10 June 2005; accepted 12 June 2005

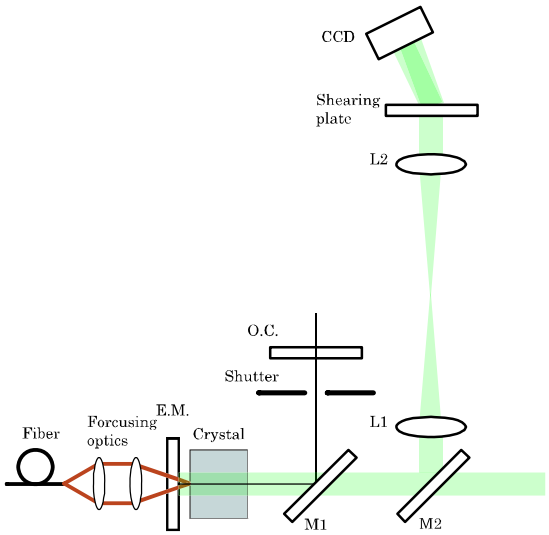

Fig. 3. Experimental setup for thermal lens measurement.;L1 and L2 are lenses with a focal length of 300 mm. And they form an imaging optics, and produce an image of a crystal face onto a CCD camera. The distance between the crystal and L1 is 300 mm. The distance between L2 and a CCD camera is 300 mm.

(a) (b)

Fig. 4. Fringes (a) with and (b) without lasing at 8 W of absorbed power

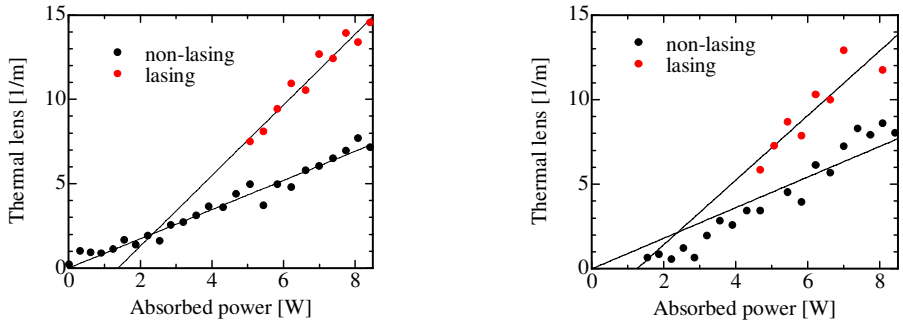

(a) $Nd:YVO_4$ (b) $Nd:GdVO_4$

Fig. 5. Thermal lens power of (a) $Nd:YVO_4$ and (b) $Nd:GdVO_4$ crystal as a function of absorbed power.

The measured thermal lens power as a function of the absorbed pump power is plotted in Fig. 5. In the case of $Nd:YVO_4$, the thermal lens power without laser action was proportional to the absorbed pump power with a slope of 0.9 m^{-1}/W. Once the laser turned on, the slope

#7562 - $15.00 USD Received 23 May 2005; revised 10 June 2005; accepted 12 June 2005

increased to 2.1 m^{-1}/W. This value was 2 times larger than the slope without laser action. In order to confirm the measured value of the thermal lens power, we also investigated the cavity stability. When the cavity length was longer than 13cm, saturation of output power occurred at a higher pump power of 7 W (Fig. 6). This phenomenon means that the focal length of thermal lens at a pump power of 7 W is shorter than 13 cm. This criterion for the focal length of thermal lens is consistent with the value measured by the interferometric technique.

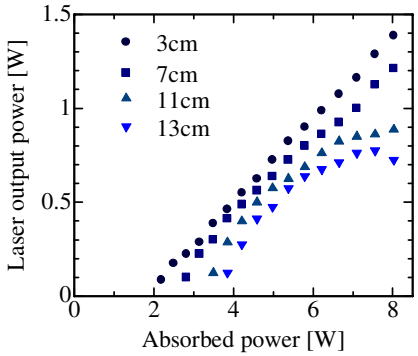

Fig. 6. Laser output of Nd:YVO_4 crystal with different cavity length

We also measured it for Nd:$GdVO_4$ crystal. The slope ratio of thermal lens with and without laser action was 2.1. Nd:$GdVO_4$ shows comparable thermal lens with Nd:YVO_4, though Nd:$GdVO_4$ has good thermal conductivity in comparison with Nd:YVO_4. In general, thermal lens is proportional to the product of thermal conductivity and (dn/dT). The unexpected large thermal lens in Nd:$GdVO_4$ is due to its large thermo-optic coefficient (dn/dT) [10,11].

The large increase in thermal loading with 1.3 μm laser action is due to a relatively large quantum energy defect between the pump and laser photons as well as strong ESA (a process in which the excited ions lying in the upper laser level transit to the higher excited level through 1.3 μm lasing photon absorption).

ESA is evidenced by visible emission from the pumped crystal due to visible fluorescence from higher lying levels such as $^4G_{7/2}$. We observed the fluorescence by using a spectrometer and an intensified CCD camera. The fluorescence spectrum is shown in Fig. 7.

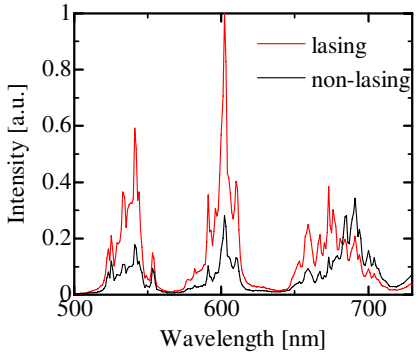

Fig. 7. Fluorescence spectrum in visible region with 8 W absorbed power (Nd:YVO_4)

Above the threshold, three strong peaks appeared around 540 nm, 600 nm and 670 nm, while below the threshold these peaks were much weaker. These correspond to the $^4G_{7/2} \rightarrow {}^4I_{9/2}$, $^4G_{7/2} \rightarrow {}^4I_{11/2}$ and $^4G_{7/2} \rightarrow {}^4I_{13/2}$ transitions, respectively. Their intensities with laser action were much stronger than them without laser action. Figure 8 shows fluorescence intensity

#7562 - $15.00 USD Received 23 May 2005; revised 10 June 2005; accepted 12 June 2005

corresponding to radiative transition of $^4G_{7/2} \rightarrow {}^4I_{11/2}$ as a function of absorbed power. The fluorescence intensity with 1.3μm laser action was 3-times larger than that without laser action at the maximum pump level. These show ESA contributes significantly to the fractional thermal loading with 1.3μm laser action.

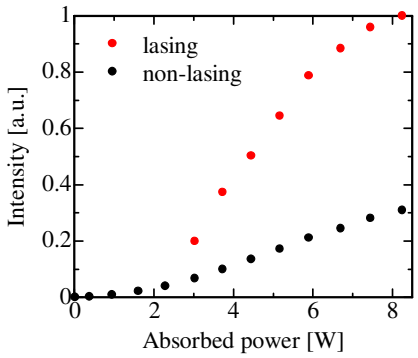

Fig. 8. Fluorescence intensity which correspond to $^4G_{7/2} \rightarrow {}^4I_{11/2}$ radiative transition as a function of absorbed power (Nd:YVO_4)

3. Discussion

The fluorescence lifetime, τ_f, as a function of Nd ions concentration is presented in Table 1.

Table 1. Fluorescence lifetime as a function of Nd ions concentration

Nd concentration (at. %)	Fluorescence lifetime (μs)	
	YVO_4	$GdVO_4$
0.4	110 [12]	-
0.5	-	107 [13]
0.9	-	97 [14]
1.0	100 [15]	95 [15]
1.1	90 [10]	-
1.2	-	90 [3]
2.0	50 [10]	44 [16]

The radiative lifetime, τ_{rad}, was estimated by using Dexter's theory [17].It was 120 μs for Nd:YVO_4 and 122 μs for Nd:$GdVO_4$.Then, we estimated the fluorescence lifetime of our crystals Nd ion concentration was 0.3 at. % in which. The value of β, the fraction of energy stored in the upper laser level that decays non-radiatively was calculated using the result,

$$\beta = \frac{1/\tau_f - 1/\tau_{rad}}{1/\tau_f}. \tag{2}$$

The fractional thermal loading without laser action η_{non} is given by,

$$\eta_{non} = 1 - \eta_q (1-\beta)\frac{\lambda_p}{\lambda_f}, \tag{3}$$

#7562 - $15.00 USD
Received 23 May 2005; revised 10 June 2005; accepted 12 June 2005

where η_q is the pump quantum efficiency, and λ_p and λ_l are the pump and laser wavelengths respectively.

The fractional thermal loading (fraction of absorbed power deposited as heat) depends on laser action. The ratio of the thermal lens powers with and without laser action was near unity at threshold. Above threshold, this ratio increased to a value of 2 for both crystals. Above the threshold, the population of the Nd^{3+} ions in the upper laser level, N_u, described by the following expression,

$$N_u \approx \frac{\eta_q P_{pump}}{c(\sigma_e + \sigma_{ESA})N_l}, \tag{4}$$

where c is the speed of light, σ_e is the stimulated emission cross-section, σ_{esa} is ESA cross-section, η_q is the pump quantum efficiency, P_{pump} is the pump photon rate, and N_l is the laser photon density, respectively. Though a part of the ions lying in $^4G_{7/2}$ decay to the ground level through a radiative process, most of them decay non-radiatively through the internal energy conversion. To simplify the model, we assumed that the radative decay rate of $^4G_{7/2}$ level is negligible. And then, the fractional thermal loading with laser action is given by,

$$\eta_{lasing} = 1 - \frac{c\sigma_e N_u}{P_{pump}} N_l \frac{\lambda_p}{\lambda_l} = 1 - \eta_q \left(\frac{\lambda_p}{\lambda_l}\right) \cdot \frac{\sigma_e}{\sigma_e + \sigma_{ESA}}, \tag{5}$$

where λ_p is the pump wavelength and λ_l is the laser wavelength, respectively. Thus, the ratio of the fractional thermal loading between with and without laser action, α, is given by,

$$\alpha = \frac{\eta_{lasing}}{\eta_{non}} = \frac{1 - \eta_q \left(\frac{\lambda_p}{\lambda_l}\right) \cdot \frac{\sigma_e}{\sigma_e + \sigma_{ESA}}}{1 - \eta_q (1-\beta)\frac{\lambda_p}{\lambda_f}}. \tag{6}$$

Substituting the physical parameters given in references [7,13,18,19], the ratios for Nd:YVO_4 and Nd:$GdVO_4$ crystals were estimated to be 2.0 and 2.2, respectively. These values are in good agreement with those measured from the thermal lens powers with and without laser action. These show that ESA for 1.3 μm laser photon should significantly increase the fractional thermal loading and as little as 40 % of the absorbed power can contribute effectively to the laser output. These results are in good agreement with the experimental slope efficiency obtained previously by 1.3 μm laser based on the Nd doped vanadates.

4. Conclusion

We have investigated the fractional thermal loading in Nd:YVO_4 and Nd:$GdVO_4$ crystals with the 1.3 μm laser action by thermal lens measurement using an interferometric method. Above threshold, the fractional thermal loading with laser action increased by a factor of 2 for both crystals. The spectroscopic measurement of the visible fluorescence from the pumped crystals confirms that the increase in the thermal loading is due to excited state absorption.

#7562 - $15.00 USD Received 23 May 2005; revised 10 June 2005; accepted 12 June 2005